A STATISTICAL APPROACH TO TEXTURE IMAGE RETRIEVAL VIA ALPHA-STABLE MODELING OF WAVELET DECOMPOSITIONS

George Tzagkarakis and Panagiotis Tsakalides

Department of Computer Science, University of Crete &
Institute of Computer Science - FORTH
ICS-FORTH, P.O. Box 1385, 711 10 Heraklion, Crete, Greece
E-mail: {gtzag, tsakalid}@ics.forth.gr

ABSTRACT

This paper addresses issues that arise in content-based information retrieval systems, which employ statistical feature extraction and similarity measurements of texture images. First, we observe that statistical distributions with heavy algebraic tails, such as the alpha-stable family, are in many cases more accurate modeling tools for the wavelet coefficients of images than families with exponential tails, such as the generalized Gaussian. Motivated by our modeling results, we extend a new wavelet-based texture retrieval method introduced recently by Do and Vetterli by computing the Kullback-Leibler distance between alpha-stable distributions. We analyze the performance of the proposed retrieval method through experimental results on a database of texture images and we compare it to the performance of the traditional approaches.

1. INTRODUCTION

Increasing agglomerations of visual information are stored in large databases, making digital image libraries more widely used. To improve the management of these databases, we need effective and precise methods to search and interact with them. For this purpose, content-based image retrieval (CBIR) from unannotated image databases has been gaining the interest of the research community.

A typical CBIR system is displayed in Figure 1. We can distinguish two major tasks, namely feature extraction (FE) and similarity measurement (SM). In the FE step, a set of features, constituting the so-called image signature, is generated to accurately represent the content of a given image. This set has to be much smaller in size than the original image while capturing as much as possible of the image information. Typical low-level image features are the shape, texture and color. During the SM step, a distance function is employed, which measures how close to a query image each image in the database is.

Recently, Do and Vetterli have introduced a statistical framework for texture retrieval in CBIR applications by jointly considering the two problems of FE and SM [1]. In their approach, the FE step becomes an ML estimator for the model parameters of the image data and the SM step computes the Kullback-Leibler distance between the model parameters. They applied this statistical framework in a wavelet-based texture retrieval application, where wavelet coefficients in each subband were independently modeled by a generalized Gaussian density (GGD).

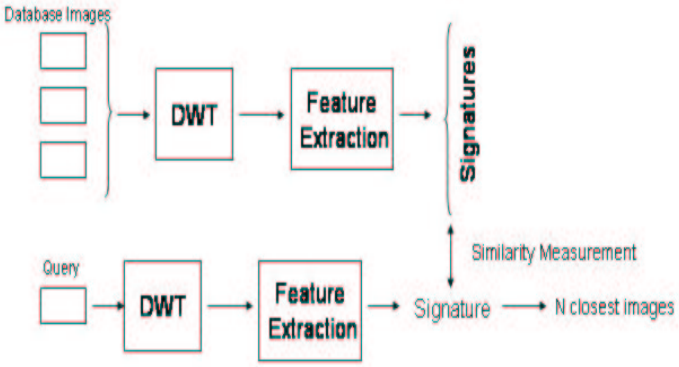

Fig. 1. A typical CBIR system.

In recent work, we have shown that successful image processing algorithms can achieve both noise reduction and feature preservation if they take into consideration the actual heavy-tailed behavior of the signal and noise densities [2, 3]. Specifically, we have shown that the subband decompositions of various types of images, including ultrasound and SAR, have non-Gaussian statistics that are best described by families of distributions with algebraic tails, such as the alpha-stable. We consequently designed Bayesian processors that exploited these statistics and had significantly improved performance in real data.

In this work, we address the CBIR problem in a statistical framework. The approach taken is similar to the method reported in [1] in that (i) texture retrieval is performed in the wavelet transform domain where wavelet coefficients in each subband are independently modeled, and (ii) texture similarity is measured by means of the Kullback-Leibler distances (KLD) between model parameters. The added value of our present work is twofold: first, we show that an often better approximation for the marginal density of coefficients at a particular subband produced by various types of wavelet transforms may be obtained by alpha-stable models; second, we calculate the KLDs between two $S\alpha S$ densities, which by itself is a novel theoretical result. Finally, we analyze the performance of the proposed retrieval method

This work was supported by the Greek General Secretariat for Research and Technology under Program ΕΠΑΝ, Codes ΗΠΑ-011 and 1308/B1/3.3.1/317/12.04.2002.

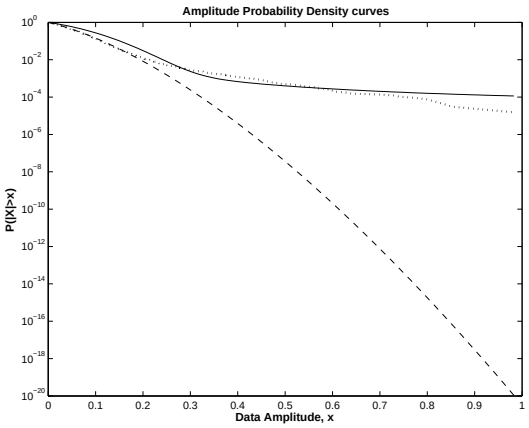

Fig. 2. Modeling of the vertical subband at the first level of decomposition of the *Flowers.0006* image with the $S\alpha S$ and the GGD depicted in solid and dashed lines, respectively. The estimated parameters for the $S\alpha S$ distribution have the values $\alpha = 0.98$, $\gamma = 0.0044$ while the GGD has parameters $\alpha = 0.0814$ and $\beta = 1.522$. The dotted line denotes the empirical APD.

through experimental results on a database of texture images and we compare it to the performance of the GGD-KLD method by Do and Vetterli.

2. STATISTICAL CHARACTERIZATION OF WAVELET SUBBAND COEFFICIENTS

In the FE step, the image is decomposed into several scales through a multiresolution analysis employing the 2-D wavelet transform [4]. The energies of the resulting wavelet coefficients identify the image texture. Our proposed method is based on the accurate modeling of the tails of the marginal distribution of the wavelet coefficients at each subband: the wavelet subband coefficients in various scales are modeled as symmetric alpha-stable ($S\alpha S$) random variables.

The $S\alpha S$ distribution, which does not have a closed-form expression except for the Cauchy and Gaussian cases, is best defined by its characteristic function. As there are multiple parameterizations of the general one-dimensional stable densities, the characteristic function can take different forms depending on the choice of the parameterization. Typical forms of the $S\alpha S$ characteristic function are [5]:

$$\phi_1(\omega) = \exp(\jmath\delta\omega - \gamma|\omega|^\alpha), \quad (1)$$

$$\phi_2(\omega) = \exp(\jmath\delta\omega - \gamma^\alpha|\omega|^\alpha), \quad (2)$$

$$\phi_3(\omega) = \exp(\jmath\delta\omega - \frac{1}{\alpha}\gamma_2^\alpha|\omega|^\alpha), \quad (3)$$

where α is the *characteristic exponent*, taking values $0 < \alpha \leq 2$, δ $(-\infty < \delta < \infty)$ is the *location parameter*, and γ, γ_2 $(\gamma,\ \gamma_2 > 0)$ are the *dispersions* of the distributions, with $\gamma_2 = \alpha^{1/\alpha}\gamma$. The $S\alpha S$ model is suitable for describing signals with heavier distribution tails than what is assumed by exponential families, like the GGD. Indeed, the $S\alpha S$ density follows an algebraic rate of decay that depends on the value of the characteristic exponent: $P(X > x) \sim c_\alpha x^{-\alpha}$. During the FE step, we estimate the $S\alpha S$ model parameters (α, γ) using the consistent maximum likelihood (ML) method described by Nolan [6], which gives reliable estimates and provides the most tight confidence intervals.

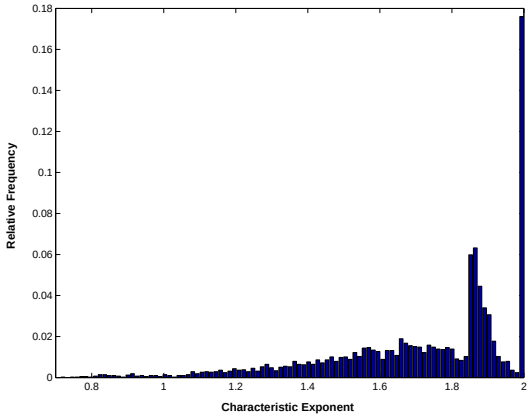

Fig. 3. Histogram of the estimated values for the characteristic exponent, α, from 448 texture images of size 128×128.

In our data modeling study, we used 28 randomly chosen textures (real-world 512×512 natural scene images) obtained from the MIT Vision Texture (VisTex) database. We divided each image into 16 128×128 subimages and we employed three levels of decomposition. The statistical fitting proceeds in two steps: First, we assess whether the data deviate from the normal distribution and we determine if they have heavy tails by employing normal probability plots. Then, we check if the data is in the stable domain of attraction by estimating the characteristic exponent, α, directly from the data and by providing the related confidence intervals. As further stability diagnostics, we employ the amplitude probability density (APD) curves ($P(|X| > x)$ that give a good indication of whether the $S\alpha S$ fit matches the data near the mode and on the tails of the distribution.

As an example, the heavy-tailed behavior of the wavelet coefficients for a given subband of the *Flowers.0006* image is depicted in Figure 2 where we compare the $S\alpha S$ and GGD fits for the selected subband. Clearly, the $S\alpha S$ density follows more closely the tail of the empirical APD than the exponentially decaying GGD. The modeling of the 28 database images (decomposed in 3 levels) produced values of the α parameter in the range between 0.7 and 2, as it is shown in the histogram of the estimated values (cf. Figure 3). We observe that for this set of images, a large fraction of the wavelet coefficients, approximately one out of two, follows statistics close to Gaussian ($1.8 \leq \alpha \leq 2$). These coefficients generally belong to the third decomposition level. On the other hand, a considerable portion of the coefficients (belonging to the first two decomposition levels) exhibits a clear heavy-tailed behavior ($\alpha \leq 1.8$).

3. SIMILARITY MEASUREMENT BETWEEN $S\alpha S$ DISTRIBUTIONS

Recent work by Do and Vetterli used generalized Gaussian distributions to model the wavelet subband coefficients. As a result, the similarity measurement step was carried out by employing the Kullback-Leibler distance between two GGDs. The overall distance between two images was defined as the sum of the KLDs between corresponding pairs

of subbands. The KLD between two GGDs has a closed-form expression [1]:

$$D(p(.;\alpha_1,\beta_1)\|p(.;\alpha_2,\beta_2)) = \log\Big(\frac{\beta_1\alpha_2\Gamma(1/\beta_2)}{\beta_2\alpha_1\Gamma(1/\beta_1)}\Big) + \Big(\frac{\alpha_1}{\alpha_2}\Big)^{\beta_2}\frac{\Gamma((\beta_2+1)/\beta_1)}{\Gamma(1/\beta_1)} - \frac{1}{\beta_1} \quad (4)$$

where $(\alpha_1,\ \beta_1)$ and $(\alpha_2,\ \beta_2)$ are the scale-shape parameter pairs of each GGD, respectively.

When considering the alpha-stable family, the KLD between two Cauchy distributions ($S\alpha S$ with $\alpha = 1$) is calculated to be

$$D(p(.;\gamma_1)\|p(.;\gamma_2)) = \log\Big(\frac{\gamma_1}{\gamma_2}\Big) + 2\frac{\gamma_1^2}{\gamma_2}\cdot\log\Big(1+\frac{\gamma_2}{\gamma_1}\Big) - \gamma_1\cdot\log 4 \quad (5)$$

where

$$p(x;\gamma) = \frac{\gamma}{\pi(x^2+\gamma^2)} \quad (6)$$

is a symmetric Cauchy density function with zero mean. Unfortunately, there is no closed-form expression for the KLD between two general $S\alpha S$ distributions, which are not Cauchy or Gaussian. To address this problem, we could employ numerical techniques for the computation of the KLD between two, numerically approximated $S\alpha S$ densities. This approach could be adequate when the image is decomposed in a small number of levels, because the number of the approximated densities is proportional to the number of these levels. In any other case, this method would significantly increase the computational burden.

In order to avoid the increased computational complexity of a numerical scheme, we applied the KLD on the normalized versions of the corresponding characteristic functions (CF). Due to the one-to-one correspondence between a $S\alpha S$ density and its associated characteristic function, we expect that the KLD between normalized CFs will be a good similarity measure between $S\alpha S$ distributions.

The normalization procedure for a characteristic function, results in its transformation into a valid probability density function. If $\phi(\omega)$ is a CF corresponding to a $S\alpha S$ distribution, then the function

$$\hat{\phi}(\omega) = \frac{\phi(\omega)}{c} \quad (7)$$

is a valid density function when

$$c = \int_{-\infty}^{\infty}\phi(\omega)\,d\omega.$$

For the parameterizations of the $S\alpha S$ CF described in the previous section, and assuming that the densities are centered at zero, i.e., $\delta = 0$, the corresponding normalized CFs are defined as:

$$\hat{\phi}_i(\omega) = \frac{\phi_i(\omega)}{c_i}, \qquad i = 1,2,3 \quad (8)$$

with

$$c_1 = \frac{2\Gamma\left(\frac{1}{\alpha}\right)}{\alpha\,\gamma^{1/\alpha}}, \quad c_2 = \frac{2\Gamma\left(\frac{1}{\alpha}\right)}{\alpha\,\gamma}, \quad c_3 = \frac{2\Gamma\left(\frac{1}{\alpha}\right)}{\alpha^{1-1/\alpha}\,\gamma_2}. \quad (9)$$

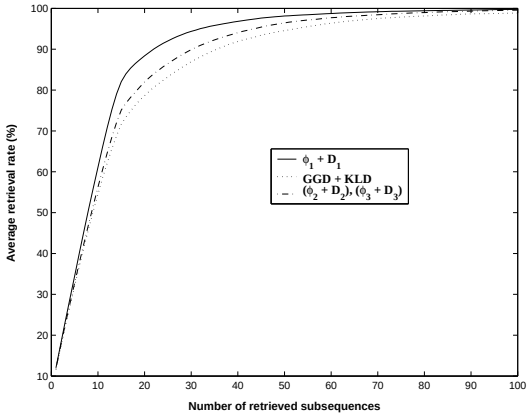

Fig. 4. Retrieval performance according to the number of top matches considered. The performance for both the $\phi_2 + D_2$ and $\phi_3 + D_3$ combinations is the same.

The promising result of the above mentioned procedure is that we have obtained closed-form expressions for normalized CFs related with $S\alpha S$ densities. By employing the KLD between a pair of normalized CFs for each one of the above three parameterizations, we obtained the following closed form expressions:

$$D_1(\hat{\phi}_1\|\hat{\phi}_2) = \ln\Big(\frac{c_2}{c_1}\Big) - \frac{1}{\alpha_1} + \frac{2\gamma_2\Gamma\left(\frac{\alpha_2+1}{\alpha_1}\right)}{c_1\alpha_1\gamma_1^{\frac{\alpha_2+1}{\alpha_1}}} \quad (10)$$

$$D_2(\hat{\phi}_1\|\hat{\phi}_2) = \ln\Big(\frac{c_2}{c_1}\Big) - \frac{1}{\alpha_1} + \Big(\frac{\gamma_2}{\gamma_1}\Big)^{\alpha_2}\cdot\frac{\Gamma\left(\frac{\alpha_2+1}{\alpha_1}\right)}{\Gamma\left(\frac{1}{\alpha_1}\right)} \quad (11)$$

$$D_3(\hat{\phi}_1\|\hat{\phi}_2) = \ln\Big(\frac{c_2}{c_1}\Big) - \frac{1}{\alpha_1} + \Big(\frac{\gamma_2}{\gamma_1}\Big)^{\alpha_2}\cdot\frac{\alpha_1^{\alpha_2/\alpha_1}\,\Gamma\left(\frac{\alpha_2+1}{\alpha_1}\right)}{\alpha_2\,\Gamma\left(\frac{1}{\alpha_1}\right)} \quad (12)$$

where $(\alpha_i,\ \gamma_i)$ are the parameters of the CF, $\phi_i(\omega)$, and c_i is its normalizing factor.

4. EXPERIMENTAL RESULTS

The proposed retrieval scheme is first applied on one-dimensional synthetic data, and then on a set of texture images found in the VisTex database.

4.1. 1-D Synthetic Sequences

First, we test the proposed KLD-$S\alpha S$ scheme with 1-D synthetic data in order to validate the distance measures (10)-(12) of Section 3. The generated data set consists of 120 1-D synthetic $S\alpha S$ sequences, with the parameters α and γ spanning the ranges [0.45, 1.5] and [0.1, 3], respectively. We split each sequence into 16 subsequences constructing a new data set of 1920 1-D signals. Then, we estimated the parameters of these sequences by considering them first as $S\alpha S$ random variables and second as generalized Gaussian random variables. In the retrieval stage, a query signal is any one of 1920 sequences in the database. The relevant

Methods			
GGD + KLD	$\phi_1 + D_1$	$\phi_2 + D_2$	$\phi_3 + D_3$
71.6504	82.0638	75.0944	75.0944

Table 1. Average retrieval rate (%) in the top 15 matches.

Filters	Methods - Level 1		
	GGD + KLD	$\phi_1 + D_1$	$\phi_2 + D_2$
db2	66.99	73.63	67.19
db4	65.43	75.29	66.11
Filters	Methods - Level 2		
	GGD + KLD	$\phi_1 + D_1$	$\phi_2 + D_2$
db2	67.28	73.34	68.55
db4	67.67	74.90	68.55
Filters	Methods - Level 3		
	GGD + KLD	$\phi_1 + D_1$	$\phi_2 + D_2$
db2	67.77	75	69.14
db4	67.96	77.93	70.80

Table 2. Average retrieval rates (%) for the selected subset of images in the top 15 matches, using Daubechies' filters db2, db4, and for 3 decomposition levels.

sequences for each query are defined as the other 15 subsequences from the same original sequence. Table 1 shows the comparison in performance in terms of average percentages of retrieving relevant subsequences in the top 15 matches, for each one of the above described similarity measures.

Figure 4 shows the average percentages of retrieving relevant subsequences as a function of the number of top matches. We observe that the combination of the $S\alpha S$ parameters with the derived KLD distances (D_i, $i = 1, 2, 3$) converges faster than the GGD-KLD method. Also, the combinations $\phi_2 + D_2$, $\phi_3 + D_3$ exhibit the same performance in all cases. In addition, the $\phi_1 + D_1$ variant gives the best convergence among the three parameterizations. Of course, this synthetic data being $S\alpha S$ it comes as no surprise the better performance of the $S\alpha S$-KLD method. The point we make is that when the data do follow algebraic tails, the new scheme can decrease the retrieval error rate.

4.2. Texture Images

In this experiment, we compared the performance of the proposed similarity measures by applying them on the set of 28 images obtained from the VisTex database. From these images we generated a database of subimages according to the procedure described in Section 2. The relevant subimages for each query are defined as the other 15 subimages from the same original image. Then, we employed the 2-D DWT with different decomposition levels and filters.

We first tested the retrieval performance in a subset of the images with fairly heavy-tailed wavelet decompositions, which had estimated feature values ($S\alpha S$ parameters α and γ) falling further apart than the range of the associated estimation confidence intervals. One should expect that the tighter the confidence intervals, the better the estimation of the features, and the better the retrieving performance. Indeed, Table 2 shows that the $\phi_1 + D_1$ variant of the $S\alpha S$-KLD method has a 7 to 10 % improved retrieval rate than the GGD-KLD method.

Filters	Methods - Level 1		
	GGD + KLD	$\phi_1 + D_1$	$\phi_2 + D_2$
db2	69.51	50.96	57.09
db4	70.46	53.14	56.90
Filters	Methods - Level 2		
	GGD + KLD	$\phi_1 + D_1$	$\phi_2 + D_2$
db2	70.74	58.52	61.61
db4	71.14	61.03	63.07
Filters	Methods - Level 3		
	GGD + KLD	$\phi_1 + D_1$	$\phi_2 + D_2$
db2	71.60	60.70	63.22
db4	72.03	63.04	65.02

Table 3. Average retrieval rates (%) for the selected set of images in the top 15 matches, using Daubechies' filters db2, db4, and for 3 decomposition levels.

When we considered all 28 images, the performance of our proposed similarity measures was lower compared with the performance of the GGD model. The reason is two-fold. First, as we observe in Figure 3, one out of two features for this data set has almost Gaussian statistics ($\alpha > 1.8$). Even more important, we observed that large confidence intervals in the estimation of the characteristic exponent values permit the values of α between two distinct images to fall very close to each other. Hence, inaccuracies in the feature extraction process impede the similarity measurement task of texture retrieval.

In conclusion, in this paper we extended a recently introduced wavelet-based texture retrieval method by computing Kullback-Leibler distance measures between alpha-stable distributions. Preliminary experimental results on a database of texture images showed that the proposed scheme can be used successfully when the data follow algebraic tails.

5. REFERENCES

[1] M. N. Do and M. Vetterli, "Wavelet-based texture retrieval using generalized Gaussian density and Kullback-Leibler distance," *IEEE Trans. Image Processing*, vol. 11, pp. 146–158, Feb. 2002.

[2] A. Achim, A. Bezerianos, and P. Tsakalides, "Novel Bayesian multiscale method for speckle removal in medical ultrasound images," *IEEE Trans. Med. Imag.*, vol. 20, pp. 772–783, Aug. 2001.

[3] A. Achim, P. Tsakalides, and A. Bezerianos, "SAR image denoising via Bayesian wavelet shrinkage based on heavy-tailed modeling," *IEEE Trans. Geosc. and Rem. Sens.*, vol. 41, pp. 1773–1784, Aug. 2003.

[4] S. G. Mallat, "A theory for multiresolution signal decomposition: The wavelet representation," *IEEE Trans. Pattern Anal. Machine Intell.*, vol. 11, pp. 674–692, July 1989.

[5] J. P. Nolan, "Parameterizations and modes of stable distributions," *Statistics & Probability Letters*, no. 38, pp. 187–195, 1998.

[6] J. P. Nolan, "Numerical calculation of stable densities and distribution functions," *Commun. Statist.-Stochastic Models*, vol. 13, pp. 759–774, 1997.